

University of Groningen

## The electronic structure of the metastable layer compound 1T-CrSe<sub>2</sub>

Fang, C.M.; Groot, R.A. de; Wiegers, G.A.; Haas, C.; vanBruggen, C.F.; deGroot, R.A.

*Published in:*  
Journal of Physics%3A Condensed Matter

*DOI:*  
[10.1088/0953-8984/9/46/015](https://doi.org/10.1088/0953-8984/9/46/015)

**IMPORTANT NOTE:** You are advised to consult the publisher's version (publisher's PDF) if you wish to cite from it. Please check the document version below.

*Document Version*  
Publisher's PDF, also known as Version of record

*Publication date:*  
1997

[Link to publication in University of Groningen/UMCG research database](#)

### *Citation for published version (APA):*

Fang, C. M., Groot, R. A. D., Wiegers, G. A., Haas, C., vanBruggen, C. F., & deGroot, R. A. (1997). The electronic structure of the metastable layer compound 1T-CrSe<sub>2</sub>. *Journal of Physics%3A Condensed Matter*, 9(46), 10173-10184. <https://doi.org/10.1088/0953-8984/9/46/015>

### **Copyright**

Other than for strictly personal use, it is not permitted to download or to forward/distribute the text or part of it without the consent of the author(s) and/or copyright holder(s), unless the work is under an open content license (like Creative Commons).

The publication may also be distributed here under the terms of Article 25fa of the Dutch Copyright Act, indicated by the "Taverne" license. More information can be found on the University of Groningen website: <https://www.rug.nl/library/open-access/self-archiving-pure/taverne-amendment>.

### **Take-down policy**

If you believe that this document breaches copyright please contact us providing details, and we will remove access to the work immediately and investigate your claim.

*Downloaded from the University of Groningen/UMCG research database (Pure): <http://www.rug.nl/research/portal>. For technical reasons the number of authors shown on this cover page is limited to 10 maximum.*

# The electronic structure of the metastable layer compound 1T-CrSe<sub>2</sub>

C M Fang, C F van Bruggen, R A de Groot, G A Wiegers and C Haas

Chemical Physics, Materials Science Centre, University of Groningen, Nijenborgh 4, 9747 AG Groningen, The Netherlands

Received 17 February 1997

**Abstract.** The electronic structure of the metastable compound 1T-CrSe<sub>2</sub> ( $a = 3.399$  Å,  $c = 5.911$  Å, space group  $P\bar{3}m1$ ) was calculated with and without spin polarization using the LSW method. The energy is 0.29 eV/mol CrSe<sub>2</sub> lower for the spin-polarized calculation. The total magnetic moment of  $+2.44 \mu_B$  on Cr consists of  $3.28 \mu_B$  in spin-up and  $0.84 \mu_B$  in spin-down states; the total number of 3d electrons on Cr is 4.12, much greater than expected for Cr(IV) 3d<sup>2</sup>. The Cr 3d-based bands overlap the selenium 4p-based valence band which implies strong covalency of the Cr–Se bonding. At the Fermi level there are electrons and holes with Cr 3d character, and holes with Se 4p character. The results clearly indicate the reduction of the cations and the presence of holes in the Se 4p valence band. CrSe<sub>2</sub> is a magnetic metal. Similar calculations for VSe<sub>2</sub> showed a very small energy difference between the magnetic and non-magnetic states, indicating that VSe<sub>2</sub> is a non-magnetic metal.

## 1. Introduction

Some of the early transition metal dichalcogenides, viz. VS<sub>2</sub>, CrS<sub>2</sub> and CrSe<sub>2</sub>, do not exist in a stable state. However, they can be obtained as metastable in the Cd(OH)<sub>2</sub> type structure (as the stable compounds TiS<sub>2</sub>, TiSe<sub>2</sub>, VSe<sub>2</sub>, etc) by topotactic oxidation (deintercalation) at ambient temperature of alkali metal intercalates MTX<sub>2</sub> (M = alkali metal). Murphy *et al* [1] were the first to prepare metastable VS<sub>2</sub> with the Cd(OH)<sub>2</sub> structure (1T-VS<sub>2</sub>) by the oxidation of LiVS<sub>2</sub> with I<sub>2</sub> dissolved in acetonitrile. Deintercalation of MTX<sub>2</sub> consists of diffusion of the alkali metal ions out of the space between TX<sub>2</sub> sandwiches and reaction at the solid–liquid interface; in some cases (not for LiVS<sub>2</sub>) this process is accompanied by parallel shifts of the TX<sub>2</sub> sandwiches. Transition to the stable state (T<sub>2</sub>X<sub>3</sub> and X) does not occur at ambient temperature because of the high activation energy for this process.

Why are VS<sub>2</sub>, CrS<sub>2</sub> and CrSe<sub>2</sub> not stable? When going to the right of the periodic table the d levels progressively decrease in energy and may enter the sulphur or selenium p valence band. With sulphur and selenium a maximum oxidation state of four is found for Ti, Zr, Hf. In the case of TiS<sub>2</sub> the empty d band lies slightly above the valence band; TiSe<sub>2</sub> is a semi-metal. When an empty d level lies below the p valence band, the d level will be filled at the expense of the valence band and holes will appear in the top of the valence band, which means that the cations M<sup>4+</sup> are reduced and the anions X<sup>2-</sup> are oxidized. At the same time the overlap of the chalcogen p-based bands with the metal d-based bands implies strong covalency of the bonding. The ionic formula M<sup>3+</sup>X<sup>-</sup>X<sup>2-</sup> may approximately describe the products of the internal redox reaction in the metastable compounds VS<sub>2</sub>, CrS<sub>2</sub> and CrSe<sub>2</sub>. The remarkable behaviour of the unit-cell dimensions in the series 1T-TiSe<sub>2</sub>,

**Table 1.** Unit-cell dimensions,  $c/a$ ,  $z$  coordinate of Se, unit-cell volume and the metal–selenium bond lengths of 1T-TiSe<sub>2</sub>, 1T-VSe<sub>2</sub> and 1T-CrSe<sub>2</sub> at 300 K. The space group is  $P\bar{3}m1$  (No 164).

	$a$ (Å)	$c$ (Å)	$c/a$	$z$	$V$ (Å <sup>3</sup> )	M–Se (Å)
TiSe <sub>2</sub>	3.535	6.004	1.698	0.255 04	64.98	2.538 [16]
VSe <sub>2</sub>	3.352	6.104	1.821	0.256 65	59.40	2.465 [14]
CrSe <sub>2</sub>	3.399	5.911	1.738	0.25	59.14	2.456 [7]

1T-VSe<sub>2</sub>, 1T-CrSe<sub>2</sub> (table 1) is connected in some way to changes in covalency and redox state. A further reduction of the cations to  $M^{2+}$  and oxidation of the anions to  $X_2^{2-}$  pairs has occurred for MnS<sub>2</sub> and MnSe<sub>2</sub> with pyrite or marcasite structures.

Participation of the d electrons in metal–metal bonding and consequently distortion of the Cd(OH)<sub>2</sub> structure is particularly strong for the 4d and 5d transition metal dichalcogenides. 1T-TaS<sub>2</sub> (Ta 5d<sup>1</sup>) shows David-star shaped clusters of 13 Ta atoms [2]. Zig-zag chains of the transition metal atoms are present in  $\beta$ -MoTe<sub>2</sub> (Mo 4d<sup>2</sup>) [3]. In TcX<sub>2</sub> (Tc 4d<sup>3</sup>) and ReX<sub>2</sub> (Re 5d<sup>3</sup>) the metal atoms are clustered in diamond chains of four-atom clusters [4]. Participation of the d electrons in metal–metal bonding leads to strong metal–metal bonds for the 4d and 5d compounds and to much weaker bonds for the 3d transition metal compounds; e.g. in 1T-VSe<sub>2</sub> (V 3d<sup>1</sup>) the distortion of the Cd(OH)<sub>2</sub> structure occurs at low temperature (110 K and 80 K) with presumably small displacements of the V atoms [5]. 1T-CrSe<sub>2</sub> shows a remarkable temperature dependence of the unit-cell dimensions and a transition at about 180 K which may be due to clustering of the metal atoms (see below).

1T-CrSe<sub>2</sub> was prepared first by Schwarz [6] by oxidation of KCrSe<sub>2</sub> in H<sub>2</sub>O or diluted acid. Van Bruggen *et al* [7] prepared 1T-CrSe<sub>2</sub> by oxidation of KCrSe<sub>2</sub> in an oxygen and water free solution of iodine in acetonitrile. KCrSe<sub>2</sub> has the NaCrSe<sub>2</sub> structure,  $a = 3.80$  Å,  $c = 21.19$  Å, space group  $R\bar{3}m$  [8]; deintercalation is accompanied by parallel shifts of the CrSe<sub>2</sub> sandwiches and stacking faults may therefore be present. 1T-CrSe<sub>2</sub> has the Cd(OH)<sub>2</sub> structure,  $a = 3.399$  Å,  $c = 5.911$  Å at 300 K, space group  $P\bar{3}m1$  (from powder) [7]. Unit-cell dimensions ranging from 3.38 to 3.41 Å for the  $a$  axis and 5.89 to 5.92 Å for  $c$  were found by Schwarz [6] for different experimental conditions (obtained as such and heated in vacuum). The thermal behaviour was investigated by van Bruggen *et al* [7]. X-ray powder diffraction showed that on heating the compound irreversibly transforms at about 625 K (DTA) into Cr<sub>2</sub>Se<sub>3</sub> and Se. In the temperature range 180–625 K the thermal expansion is negative for the  $c$  axis and strongly positive for the  $a$  axis;  $c$  decreases from 5.95 Å at 180 K to 5.85 Å at 550 K. The  $c/a$  ratio is 1.74 at 300 K and 1.76 at 180 K. At about 180 K a reversible transition takes place with a decrease of 1% in  $c$  and a small increase in  $a$ ; the cell volume decreases therefore by about 1%. Small thermal effects of this reversible transition were noticed at 164 and 186 K using DTA. Below 180 K some weak extra reflections are present in the powder pattern; however, these could not be indexed on the basis of a simple (e.g.  $a\sqrt{3} \times a\sqrt{3}$ ) supercell. The origin of the negative thermal expansion of the  $c$  parameter and the transition at 180 K is not clear. Van Bruggen *et al* [7] suggest a random clustering of the metal atoms, increasing in the range 550–180 K. This clustering would cause a buckling of the sandwiches and an increase of the  $c$  from 500 to 180 K; long-range order of the clustering was assumed to occur below 180 K.

The electronic structure of 1T-CrSe<sub>2</sub> has been calculated by Myron [9] using a semi-empirical method in which the exchange potential was adjustable. Yoshida and Motizuki [10] obtained the band structure of 1T-CrSe<sub>2</sub> by simply using the band structure of TiSe<sub>2</sub> and taking into account only the different number of 3d electrons. In both calculations

spin polarization was not included, and the calculations were semi-empirical and not self-consistent. An *ab initio* band structure calculation of 1T-VSe<sub>2</sub> and the effect of the change in the  $c/a$  ratio at constant  $a$  and the sandwich height parameter  $z$  (coordinate of Se) was published by Zunger and Freeman [11].

In this paper we report *ab initio* band structure calculations of 1T-CrSe<sub>2</sub> with and without magnetic spin arrangements using the LSW method. The results are compared with similar calculations for 1T-VSe<sub>2</sub> and with the previous calculations for 1T-TiSe<sub>2</sub>, 1T-VSe<sub>2</sub> and 1T-CrSe<sub>2</sub>.

## 2. Band structure calculations

*Ab initio* band structure calculations were performed with the localized spherical wave (LSW) [12] method using a scalar-relativistic Hamiltonian. We used local-density exchange–correlation potentials [13] inside space-filling, and therefore overlapping, Wigner–Seitz spheres around the atomic constituents. The self-consistent calculations were carried out including all core electrons. The unit-cell dimensions of CrSe<sub>2</sub> were those at 300 K found by van Bruggen *et al* [7] and given in table 1; the  $z$  parameter of Se was given the value 0.25. An empty sphere was put at the octahedral site in the van der Waals gap (0, 0, 0.5). Similar calculations were performed for 1T-VSe<sub>2</sub>. Unit-cell dimensions and the  $z$  parameter of Se were those from [7, 14] (table 1). Iterations were performed with  $k$  points distributed uniformly in the irreducible part of the first Brillouin zone (BZ), corresponding to a volume of the BZ per  $k$  point of the order of  $5 \times 10^{-5} \text{ \AA}^{-3}$ . Self-consistently was assumed when the changes in the local partial charges in each atomic sphere decreased to the order of  $10^{-5}$ .

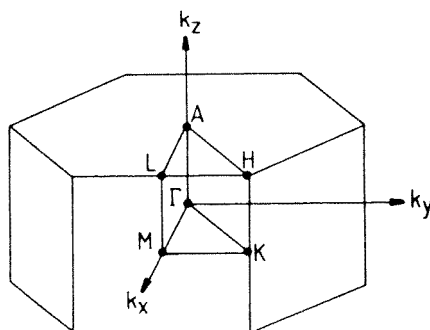
In the construction of the LSW basis [12, 15], the spherical waves were augmented by solutions of the scalar-relativistic radial equations indicated by the atomic-like symbols 4s, 4p and 3d corresponding to the valence levels of the parent elements V, Cr and Se. The internal  $l$  summation used to augment a Hankel function at surrounding atoms was extended to  $l = 3$ , resulting in the use of 4f orbitals for V, Cr and Se. When the crystal is not very densely packed, as is the case of the layered compounds CrSe<sub>2</sub> and VSe<sub>2</sub>, it is necessary to include empty spheres in the calculations. The functions 1s and 2p, and 3d as an extension were used for the empty spheres.

## 3. Electronic structure of CrSe<sub>2</sub> and VSe<sub>2</sub>

The electronic structure of CrSe<sub>2</sub> was calculated with and without spin polarization. From table 2, which lists the input parameters and calculation results (electronic configuration, variational energy and magnetic moment per Cr) it is seen that the variational energy is lower for the ferromagnetic than for the non-magnetic state by 0.29 eV per mol CrSe<sub>2</sub>. This indicates that CrSe<sub>2</sub> is a magnetic compound with local magnetic moments at the Cr atoms. Calculations performed for different magnetic ordering show that an intralayer antiferromagnetic and interlayer antiferromagnetic coupling type of ordering has the lowest energy (about 40 meV lower than the ferromagnetic state). This antiferromagnetic ordering is described in an  $a \times a\sqrt{3} \times 2c$  unit cell. Cr moments at (0, 0, 0) and  $(\frac{1}{2}, \frac{1}{2}, 0)$  as well as those at  $(0, 0, \frac{1}{2})$  and  $(\frac{1}{2}, \frac{1}{2}, \frac{1}{2})$  are in opposite directions. Cr moments at (0, 0, 0) and  $(0, 0, \frac{1}{2})$  are in opposite directions. Other more complicated antiferromagnetic structures are discussed in section 5. The influence of the magnetic ordering on the electronic structure, i.e. on the density of states and the dispersion of the energy bands, is small. We therefore only report

**Table 2.** Input parameters and results for the non-magnetic and magnetic band structure calculation of CrSe<sub>2</sub>.  $R_{WS}$  represents the Wigner–Seitz radii.

Atom	$x$	$y$	$z$	$R_{WS}$ (Å)	Electronic configuration
Non-magnetic calculation for CrSe <sub>2</sub>					
Cr 1a	0	0	0	1.1877	[Ar]4s <sup>0.22</sup> 4p <sup>0.25</sup> 3d <sup>4.12</sup> 4f <sup>0.02</sup>
Se 2d	1/3	2/3	0.25	1.7532	[Ar]4s <sup>1.93</sup> 4p <sup>4.11</sup> 4d <sup>0.35</sup> 4f <sup>0.13</sup>
V <sub>a</sub> 1b	0	0	0.5	1.1877	1s <sup>0.12</sup> 2p <sup>0.15</sup> 3d <sup>0.08</sup>
Variational energy = −11 804.918 391 Ryd					
Magnetic calculation for CrSe <sub>2</sub>					
Cr 1a	0	0	0	1.1877	[Ar]4s <sup>0.12</sup> 4p <sup>0.13</sup> 3d <sup>3.28</sup> 4f <sup>0.01</sup> (up)
					[Ar]4s <sup>0.10</sup> 4p <sup>0.12</sup> 3d <sup>0.84</sup> 4f <sup>0.01</sup> (down)
Se 2d	1/3	2/3	0.25	1.7532	[Ar]4s <sup>0.96</sup> 4p <sup>1.96</sup> 4d <sup>0.18</sup> 4f <sup>0.08</sup> (up)
					[Ar]4s <sup>0.96</sup> 4p <sup>2.20</sup> 4d <sup>0.13</sup> 4f <sup>0.04</sup> (down)
V <sub>a</sub> 1b	0	0	0.5	1.1877	1s <sup>0.12</sup> 2p <sup>0.15</sup> 3d <sup>0.07</sup> (up + down)
Total moment = 2.1695 $\mu_B$					
Variational energy = −11 804.939 477 Ryd					

**Figure 1.** Brillouin zone and high-symmetry points for 1T-CrSe<sub>2</sub> and 1T-VSe<sub>2</sub>.

the electronic structure of the ferromagnetic CrSe<sub>2</sub>. The total electronic configuration (spin up + spin down) was found to be the same for the magnetic and the non-magnetic state. The magnetic moments in the ferromagnetic state are Cr = +2.44  $\mu_B$ , Se = −0.15  $\mu_B$  (mainly in 4p), V<sub>a</sub> = 0  $\mu_B$ . The moment on Cr consists of 3.28  $\mu_B$  in spin-up and 0.84  $\mu_B$  in spin-down electrons. The total number of 3d electrons on Cr is 4.12, far from 2 as expected for Cr(IV) 3d<sup>2</sup>. The charges on the atoms and vacancy are Cr = +1.39, Se = −0.52 and V<sub>a</sub> = −0.35. Not too much attention should be paid to these charges since they depend on the choice of the Wigner–Seitz radii. Calculations with and without spin polarization were performed for 1T-CrSe<sub>2</sub> for slightly different unit-cell parameters, e.g. with the same  $a$ , but  $c$  increased by 3%; with the same  $c$ , but  $a$  increased by 3%; with the same  $a$  and  $c$ , but with  $z = 0.24$  or  $z = 0.26$ . The calculations show small changes of the electronic structure, but in all cases the ferromagnetic state is more stable than the non-magnetic state.

The Brillouin zone (BZ) of 1T-CrSe<sub>2</sub> is shown in figure 1, the density of states (DOS) of ferromagnetic CrSe<sub>2</sub> in figure 2. The energy bands are shown in figure 3(a) for spin-up and in figure 3(b) for spin-down states. Table 3 lists the eigenvectors, symmetry and the dominant orbital character at  $\Gamma$  in the BZ.

The two Se 4s states (valence band 2, VB2) are clearly separated from the valence band (VB1), consisting of Se 4p states, by a gap of about 6.5 eV for both spin-up and spin-down

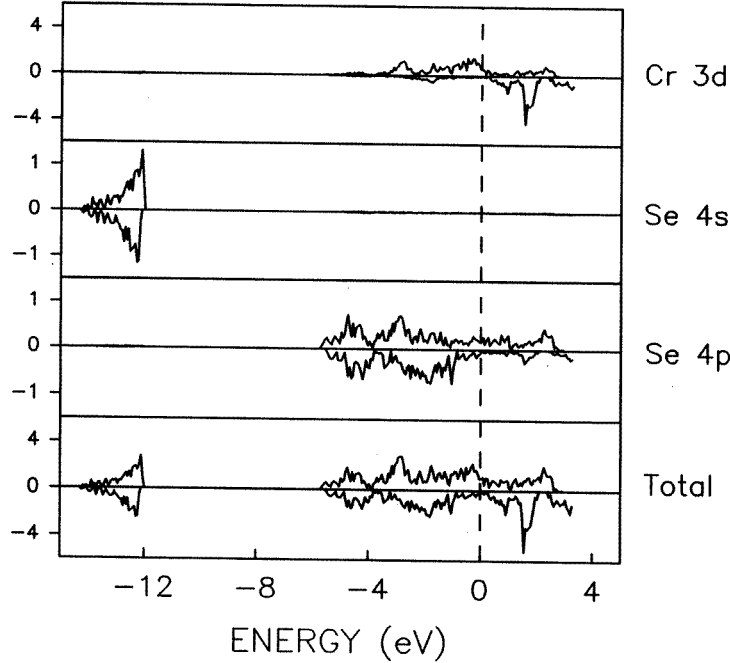


**Figure 2.** Partial and total density of states (in states/eV) of ferromagnetic 1T-CrSe<sub>2</sub>. The positive and negative parts represent the density for spin-up and spin-down electrons respectively. The Fermi level is at zero energy.

**Table 3.** Energies, symmetry and dominant orbital character (OC) at point  $\Gamma$  for the spin-polarized calculations of ferromagnetic 1T-CrSe<sub>2</sub>, and for non-magnetic 1T-VSe<sub>2</sub>. 3d\* represents 3d<sub>xz</sub>, 3d<sub>yz</sub>, 3d<sub>xy</sub>, 3d<sub>x<sup>2</sup>-y<sup>2</sup></sub>.

1T-CrSe <sub>2</sub> (spin up)			1T-CrSe <sub>2</sub> (spin down)			1T-VSe <sub>2</sub>		
<i>E</i> (eV)	Symm.	OC	<i>E</i> (eV)	Symm.	OC	<i>E</i> (eV)	Symm.	OC
-14.26	1 <sup>+</sup>	Se 4s	-14.35	1 <sup>+</sup>	Se 4s	-14.36	1 <sup>+</sup>	Se 4s
-12.76	2 <sup>-</sup>	Se 4s	-12.90	2 <sup>-</sup>	Se 4s	-13.06	2 <sup>-</sup>	Se 4s
-5.78	1 <sup>+</sup>	Se 4p <sub>z</sub>	-5.62	1 <sup>+</sup>	Se 4p <sub>z</sub>	-5.75	1 <sup>+</sup>	Se 4p <sub>z</sub>
-2.84	3 <sup>+</sup>	Se 4p <sub>x</sub> , p <sub>y</sub>	-1.74	3 <sup>+</sup>	Se 4p <sub>x</sub> , p <sub>y</sub>	-2.05	3 <sup>+</sup>	Se 4p <sub>x</sub> , p <sub>y</sub>
-1.31	3 <sup>+</sup>	Cr 3d*	+0.37	2 <sup>-</sup>	Se 4p <sub>z</sub>	-0.33	1 <sup>+</sup>	V 3d <sub>z<sup>2</sup></sub>
-1.13	1 <sup>+</sup>	Cr 3d <sub>z<sup>2</sup></sub>	+0.74	1 <sup>+</sup>	Cr 3d <sub>z<sup>2</sup></sub>	-0.15	3 <sup>+</sup>	V 3d*
+0.51	2 <sup>-</sup>	Se 4p <sub>z</sub>	+0.75	3 <sup>+</sup>	Cr 3d*	+0.01	2 <sup>-</sup>	Se 4p <sub>z</sub>
+1.12	3 <sup>-</sup>	Se 4p <sub>x</sub> , p <sub>y</sub>	+0.97	3 <sup>-</sup>	Se 4p <sub>x</sub> , p <sub>y</sub>	+1.11	3 <sup>-</sup>	Se 4p <sub>x</sub> , p <sub>y</sub>
+2.61	3 <sup>+</sup>	Cr 3d	+3.47	3 <sup>+</sup>	Cr 3d*	+3.02	3 <sup>+</sup>	V 3d*

states. One of the two Se 4s bands (1<sup>+</sup>) is bonding, the other (2<sup>-</sup>) antibonding. Both states are occupied, therefore they do not contribute to the net bonding in CrSe<sub>2</sub>.

The Se 4p<sub>z</sub> band (1<sup>+</sup>) for spin-up electrons is slightly lower than for spin-down because it is pushed down by the stronger hybridization with Cr 3d<sub>z<sup>2</sup></sub>; Cr 3d<sub>z<sup>2</sup></sub> (1<sup>+</sup>) for spin-up electrons is closer in energy so that the hybridization is larger. The splitting of the Se 4p<sub>z</sub> bands (1<sup>+</sup> and 2<sup>-</sup>) is large: 6.29 eV for spin-up and 5.99 eV for spin-down electrons at  $\Gamma$ ; they show also a large and different dispersion along the  $\Gamma$ -A direction. The splitting of Se 4p<sub>z</sub> at  $\Gamma$  is due to the inter- and intra-layer interactions. The energies of the Se 4p<sub>z</sub> states which are bonding ( $\Gamma_1^+$ ) and antibonding ( $A_1^+$ ) with respect to the Se 4p<sub>z</sub>-Se 4p<sub>z</sub> interlayer

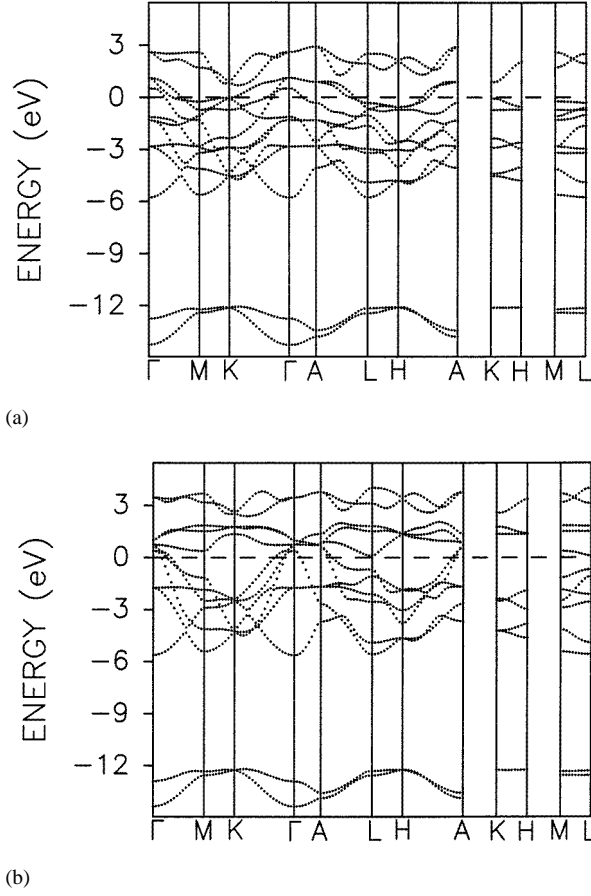


**Figure 3.** Dispersion of the energy bands for (a) spin-up and (b) spin-down electrons for ferromagnetic CrSe<sub>2</sub>.

interactions are

$$E(\Gamma_1^+) = E_0 - \Delta_{\text{interlayer}} - \Delta_{\text{intralayer}}$$

$$E(A_1^+) = E_0 + \Delta_{\text{interlayer}} - \Delta_{\text{intralayer}}$$

With  $E(\Gamma_1^+) = -5.78$  eV for spin-up and  $-5.62$  eV for spin-down electrons and  $E(A_1^+) = -4.06$  eV for spin-up and  $-3.67$  eV for spin-down electrons, one finds the interlayer interaction energy  $\Delta_{\text{interlayer}} = 0.86$  eV and  $0.98$  eV for spin-up and spin-down electrons, respectively.

The antibonding Se  $4p_x, 4p_y$  ( $3^-$ ) bands are nearly the same for spin up and spin down, indicating only a slight hybridization with Cr  $3d_{xz}, 3d_{yz}, 3d_{xy}, 3d_{x^2-y^2}$ . For the bonding Se  $4p_x, 4p_y$  ( $3^+$ ) bands there is a large difference for spin up and spin down due to a large hybridization with Cr  $3d_{xz}, 3d_{yz}, 3d_{xy}, 3d_{x^2-y^2}$  orbitals for spin-up states.

The highest two Cr  $3d$  bands ( $3^+$ , mainly  $3d_{xz}, 3d_{yz}, 3d_{xy}, 3d_{x^2-y^2}$ ), corresponding to  $e_g$  in an octahedron are nearly separated from the other bands and completely unoccupied for spin-up and spin-down states.

The lower three Cr  $3d$  bands (corresponding to  $t_{2g}$  in an octahedron) are unoccupied for spin-down and partly occupied for spin-up states. According to table 2 and figure 3 there

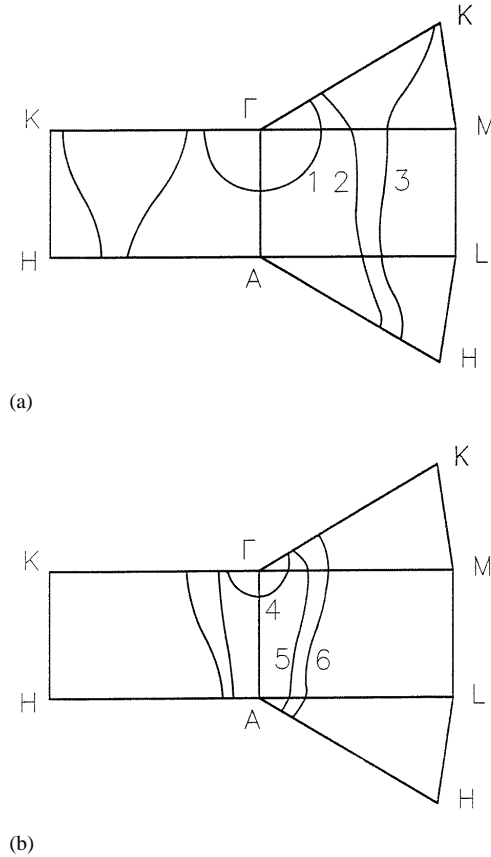


**Figure 4.** Fermi surfaces for ferromagnetic CrSe<sub>2</sub> (a) spin-up and (b) spin-down states. (1) and (4) are hole surfaces of mixed Cr (3d<sub>z<sup>2</sup></sub>)–Se (4p<sub>z</sub>) character; (2, 3) and (5, 6) are electron surfaces of mixed Cr (3d\*)–Se (4p<sub>x</sub>, p<sub>y</sub>) character.

are also 0.84 Cr 3d spin-down electrons at energies about 2.5 eV below the Fermi energy  $E_F$  because of the mixing of Se 4p<sub>x</sub>, 4p<sub>y</sub> with Cr 3d<sub>xz</sub>, 3d<sub>yz</sub>, 3d<sub>xy</sub>, 3d<sub>x<sup>2</sup>–y<sup>2</sup></sub>.

The antibonding Se 4p<sub>x</sub>, 4p<sub>y</sub> band is above  $E_F$  at  $\Gamma$  (3<sup>–</sup>) for spin-up and spin-down electrons. The same is the case for the Se 4p<sub>z</sub> band (2<sup>–</sup> at  $\Gamma$ ). This leads to hole pockets around  $\Gamma$  for spin-up and spin-down states. Holes in the Se 4p band correspond to a reduction of Cr. The formal valence of Cr is lower than Cr(IV); it is more like high-spin Cr(III) or Cr(II), as was also deduced from the total number of 3d electrons on Cr (table 2).

The Fermi surfaces are rather complex as shown in figures 4(a) and 4(b). The Fermi surface for spin-up electrons consists of (1) an ellipsoid around  $\Gamma$  (the charge carriers for this part of the Fermi surface are holes) and (2, 3) two cylinder-like sheets along  $\Gamma$ –A (the charge carriers of these sheets are electrons). The Fermi surface for spin-down electrons consists of (4) an ellipsoid around  $\Gamma$  (the charge carriers for this sheet are holes) and (5, 6) two cylinder-like sheets along  $\Gamma$ –A. The charge carriers (electrons or holes) are in all cases of mixed Cr (3d)–Se (4p) character.

The presence of holes in Se 4p<sub>z</sub> bands leads to a net covalent intralayer and interlayer bonding between Se atoms, i.e. also bonding across the van der Waals gap. The holes in the Se 4p<sub>x</sub>, 4p<sub>y</sub> bands cause covalent intralayer bonding between Se atoms.



Band structure calculations for  $\text{VSe}_2$  (input parameters and results are given in table 4) for the magnetic and non-magnetic states show a lower energy for the magnetic state; however, the energy difference is only 0.005 eV, and not significant (compare with  $\text{CrSe}_2$  where the energy difference between magnetic and non-magnetic states was 0.29 eV). The magnetic moment on V in the (ferro) magnetic state is  $0.42 \mu_B$ . In order to facilitate comparison of  $\text{CrSe}_2$  and  $\text{VSe}_2$  the dispersion curves of the non-magnetic calculations are given in figures 5 and 6. The calculations of  $\text{VSe}_2$  in general agree with those presented by Zunger and Freeman [11], not with those by Myron [9] with respect to the overlap of the metal d- and Se 4p-based bands.

**Table 4.** Input parameters and results for the band structure calculation of  $\text{VSe}_2$ .

Atom		$x$	$y$	$z$	$R_{WS}$ (Å)	Electronic configuration
V	1a	0	0	0	1.122	$[\text{Ar}]4s^{0.21}4p^{0.26}3d^{3.16}4f^{0.02}$
Se	2d	1/3	2/3	0.256 65	1.754	$[\text{Ar}]4s^{1.92}4p^{4.15}4d^{0.32}4f^{0.10}$
$V_a$	1b	0	0	0.5	1.169	$1s^{0.12}2p^{0.14}3d^{0.07}$

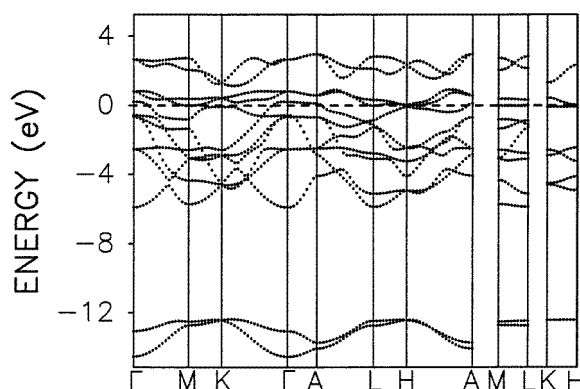


**Figure 5.** Dispersion of the energy bands for non-magnetic 1T- $\text{CrSe}_2$ .

#### 4. Comparison of the band structures of $\text{TiSe}_2$ , $\text{VSe}_2$ and $\text{CrSe}_2$

In order to understand the trends for the early transition metal diselenides  $\text{TiSe}_2$ ,  $\text{VSe}_2$  and  $\text{CrSe}_2$ , we compare the band structures of  $\text{TiSe}_2$ ,  $\text{VSe}_2$  and  $\text{CrSe}_2$ . Many band structure calculations have been performed for  $\text{TiSe}_2$ . In table 5 we compare our calculations obtained with the LSW method for  $\text{VSe}_2$ ,  $\text{CrSe}_2$  and  $\text{TiSe}_2$  [18] with results for  $\text{TiSe}_2$  and  $\text{VSe}_2$ , obtained by Zunger and Freeman with the *ab initio* LCAO method [11, 17]. For  $\text{TiSe}_2$  and  $\text{VSe}_2$  our calculations are in general agreement with those by Zunger and Freeman. However, there are some differences. The  $Td/Xp$  gaps at the high-symmetry points ( $\Gamma$ , M, L) are smaller (or more negative) in our calculations. In the calculations by Zunger and Freeman only a small number (24) of  $k$  points was used to obtain the self-consistent potential, and it is well known that this may lead to appreciable quantitative errors in the calculated energies of the bands, especially near the Fermi level and at the high-symmetry points.

The general pattern of the bands in  $\text{VSe}_2$  is qualitatively similar to that previously obtained by us for 1T- $\text{TiSe}_2$  [18] (table 5). There are important differences between the

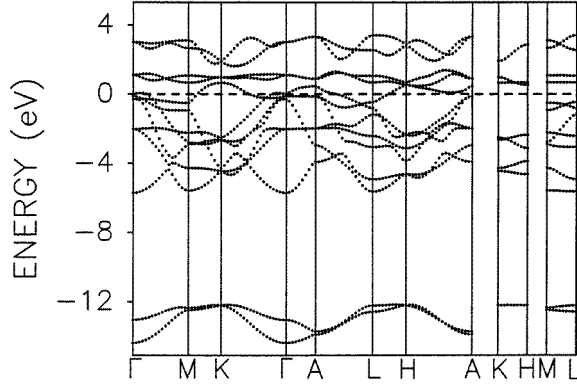


**Figure 6.** Dispersion of the energy bands for 1T-VSe<sub>2</sub>.

**Table 5.** Comparison of bandwidths and major gaps between the chalcogen p-type and metal d-type bands (denoted by an asterisk) in TiSe<sub>2</sub>, VSe<sub>2</sub>, CrSe<sub>2</sub> (non-magnetic state, nm) and CrSe<sub>2</sub> (magnetic states, spin up and spin down). Results are given in eV.

Quantity	TiSe <sub>2</sub> [17]	TiSe <sub>2</sub> [18]	VSe <sub>2</sub> [11]	VSe <sub>2</sub>	CrSe <sub>2</sub> (nm)	CrSe <sub>2</sub> (up)	CrSe <sub>2</sub> (down)
Width of VB1	5.70	5.77	5.80	6.86	6.71	6.90	6.59
Width of VB2	2.00	1.86	2.41	2.21	2.17	2.19	2.12
VB1–VB2 gap	6.92	6.78	5.98	6.39	6.41	6.30	6.66
CB1–CB2 splitting (at $\Gamma$ )	2.1	2.7	1.7	1.9	1.85	2.50	1.49
p–d gaps							
$\Gamma\Gamma^*$	0.32	–0.33	0.20	–0.34	–0.78	–1.64	0.46
$MM^*$	2.04	1.32	0.77	0.44	0.49	–0.38	1.49
$LL^*$	1.32	0.41	0.05	–0.33	0.24		
$\Gamma M^*$	0.12	–0.50	–0.47	–0.62	–1.06		
$\Gamma L^*$	–0.20	–0.80	–0.71	–0.82	–0.51		
Edge of VB1	$\Gamma_3^-$	$\Gamma_3^-$	$\Gamma_2^-$	$\Gamma_3^-$	$\Gamma_3^-$	$\Gamma_3^-$	$\Gamma_3^-$

electronic structures of TiSe<sub>2</sub>, VSe<sub>2</sub> and CrSe<sub>2</sub>, due to the different ionicity and the different  $c/a$  ratios [11]. The band structure of non-magnetic CrSe<sub>2</sub> is approximately the average of the bands for the spin-up and spin-down electrons of the ferromagnetic state. The band width of VB1 for CrSe<sub>2</sub> (6.7 eV) and VSe<sub>2</sub> (6.9 eV) is larger than for TiSe<sub>2</sub> (5.7 eV), due to the short interatomic distances in CrSe<sub>2</sub> and VSe<sub>2</sub> (table 1). The ionicity decreases from TiSe<sub>2</sub> to VSe<sub>2</sub> to CrSe<sub>2</sub>, which causes the increase of the p–d overlap (table 5). However, the bands show some non-systematical behaviour, because of the large  $c/a$  ratio for VSe<sub>2</sub> (table 1). A significant difference between the electronic structures of these compounds is that CrSe<sub>2</sub> is a magnetic metal and the others are essentially non-magnetic.

## 5. Electronic structure of CrSe<sub>2</sub> and the physical properties

The magnetic susceptibility  $\chi$  of CrSe<sub>2</sub> between 50 and 500 K is about  $2 \times 10^{-3} \text{ cm}^3 \text{ mol}^{-1}$ , and shows only a weak dependence on temperature. The weak temperature dependence indicates that CrSe<sub>2</sub> is antiferromagnetic, and not ferromagnetic or ferrimagnetic. The magnetic susceptibility of CrSe<sub>2</sub> shows at low temperature a paramagnetic tail, presumably

due to a magnetic impurity. Van Bruggen *et al* [7] suggested that this paramagnetic tail is due to the presence of 1.7 mol%  $\text{K}_{0.5}\text{CrSe}_2$  and a paramagnetic contribution from about 2.5 mol%  $\text{Cr}^{4+}$  ( $3d^2$ ) with spin-orbit coupling, due to self-intercalation of  $\text{CrSe}_2$  (Frenkel-type disorder).  $\text{K}_{0.5}\text{CrSe}_2$  is antiferromagnetic below 68 K [7]. Below 180 K  $\chi$  shows two anomalies associated with a phase transition. At high temperature (above 600 K) one observes in  $\chi$  the effects of the decomposition of  $\text{CrSe}_2$  into  $\text{Cr}_2\text{Se}_3 + \text{Se}$ .

With regard to the type of magnetic order of the local magnetic moments on Cr in  $\text{CrSe}_2$ , we remark that the Cr–Cr distance in  $\text{CrSe}_2$  is very short, i.e. 3.399 Å. The short distances in  $\text{CrSe}_2$  are (in part) due to the covalent Se–Se bonds, as a result of the presence of holes in the Se (4p) bands. The intralayer exchange interaction  $J_1$  between nearest-neighbour Cr atoms consists of a direct antiferromagnetic interaction  $J'_1$  and a ferromagnetic  $90^\circ$  superexchange interaction  $J''_1$ . The exchange interaction  $J_2$  between Cr atoms in different layers is expected to be weak and antiferromagnetic. The direct interaction  $J'_1$  depends strongly on the Cr–Cr distances: it is large for short Cr–Cr distances. These considerations explain that for compounds with short Cr–Cr distances, the paramagnetic Curie temperature  $\theta$  is negative, and that for long Cr–Cr distances  $\theta$  is positive. For example, in  $\text{LiCrS}_2$  the Cr–Cr distance is 3.464 Å and  $\theta = -276$  K [19,20], and for  $\text{NaCrSe}_2$  [22] and  $\text{KCrSe}_2$  [8] the Cr–Cr distances are 3.73 Å and 3.80 Å, and  $\theta = +108$  and  $+250$  K, respectively.  $\text{LiCrS}_2$  with a layer stacking as  $\text{CrSe}_2$  adopts the  $120^\circ$  spin structure; neighbouring layers are coupled antiferromagnetically [20]. More complicated (helical) antiferromagnetic ordering is observed in  $\text{NaCrSe}_2$  and  $\text{AgCrSe}_2$  [22]. Figure 7 also shows the relationship between  $\theta$  and the Cr–Cr distances for  $\text{ACrX}_2$  compounds ( $A = \text{Li, Na, K, Ag, Cu}$ ;  $X = \text{S, Se}$ ) [8, 19–22]. Because of the very short Cr–Cr distance in  $\text{CrSe}_2$ , we expect strong antiferromagnetic intralayer exchange interactions with  $\theta \leq -300$  K. As a consequence the magnetic structure will consist of antiferromagnetic layers. For a magnetic structure with ferromagnetic layers with a weak antiferromagnetic coupling between the layers, one would expect a very strong temperature dependence of  $\chi$ , like that observed for  $\text{KCrSe}_2$  [8].

Magnetic susceptibility data [23] for  $\text{VSe}_2$  show a temperature independent magnetic susceptibility of  $\chi = 3 \times 10^{-4} \text{ cm}^3 \text{ mol}^{-1}$  (except for a small increase of  $\chi$  at low temperature, presumably due to paramagnetic impurities). The susceptibility data show that  $\text{VSe}_2$  is a non-magnetic compound, without local magnetic moments at V, which is consistent with our band structure calculations.

The small calculated energy difference between the magnetic and non-magnetic states of  $\text{VSe}_2$  indicates that it costs very little energy to induce a magnetic moment at the V atoms. This is consistent with the fact that the observed paramagnetic susceptibility of  $\text{VSe}_2$  is very large, i.e. there is a large exchange enhancement of the Pauli paramagnetic susceptibility.

Electrical transport (resistivity, Hall effect and thermopower) and magnetic properties were measured by van Bruggen *et al* [7], on powder compacts of  $\text{CrSe}_2$ . The resistivity  $\rho$  is  $2 \times 10^{-5} \Omega \text{ m}$  at 300 K and increases to  $13 \times 10^{-5} \Omega \text{ m}$  at 4 K. The transition at 180 K is hardly visible. The Hall coefficient  $R_H$  is positive between 300 and 40 K, with a maximum at about 100 K, and becomes negative below 40 K. At 300 K  $R_H$  would correspond to 0.5 hole/Cr in a one-carrier model. The thermopower  $\alpha$  is positive. A steep rise occurs from 4 to 100 K ( $\alpha = +23 \mu\text{V K}^{-1}$  at 100 K) and a decrease in the range 100–300 K with a dip at 180 K; at 300 K  $\alpha = 10 \mu\text{V K}^{-1}$ .

The different sign of the Hall effect and the thermopower at low temperature, and the change of sign of the Hall coefficient with temperature, show that there is mixed electrical conduction in  $\text{CrSe}_2$ , i.e. by electrons and holes. This is consistent with the calculated Fermi surface (figure 4).

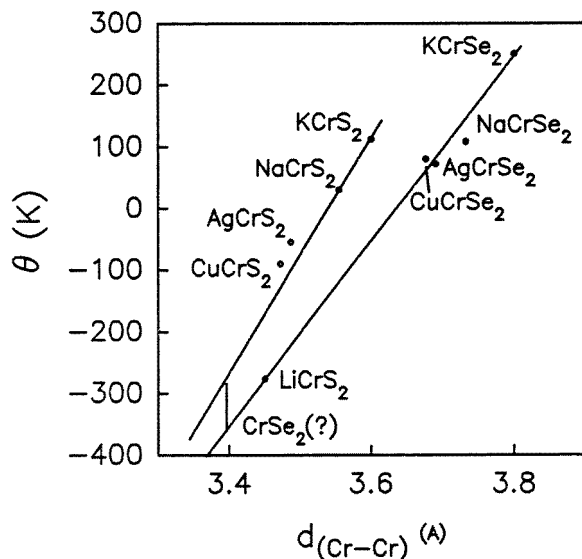


**Figure 7.** Cr–Cr distances and asymptotic Curie temperature  $\theta$  for 1T-CrSe<sub>2</sub> and some ACrX<sub>2</sub> compounds (A = Li, Na, K, Cu, Ag; X = S, Se).

## 6. Conclusions

*Ab initio* LSW spin-polarized and non-polarized band structures are calculated for CrSe<sub>2</sub> and VSe<sub>2</sub>. VSe<sub>2</sub> is non-magnetic while CrSe<sub>2</sub> is magnetic; the magnetic moment is about  $2.4 \mu_B/\text{Cr}$  ion. The valence and conduction bands are formed by the Se 4p and Cr 3d (V 3d) states; the overlap is stronger for the Cr compound. The band structure for the two spin directions of CrSe<sub>2</sub> is quite different near the Fermi level. The calculated Fermi surface shows the presence of holes in the Se (4p) bands, and both electrons and holes in the Cr (3d) bands.

## Acknowledgment

We thank Henk Bruinenberg for help in the preparation of some figures.

## References

- [1] Murphy D W, Cross C, DiSalvo F J and Waszczak J V 1977 *Inorg. Chem.* **16** 3027
- [2] Brouwer R and Jellinek F 1974 *Mater. Res. Bull.* **9** 827  
Wilson J A, Di Salvo F J and Mahajan S 1975 *Adv. Phys.* **24** 117  
Spijkerman A, de Boer J L, Meetsma A, Wiegiers G A and van Smaalen S *Phys. Rev. B* accepted for publication
- [3] Brown B E 1966 *Acta Crystallogr.* **20** 268
- [4] Fang C M, Wiegiers G A, Haas C and de Groot R A 1997 *J. Phys.: Condens. Matter* **9** 4411  
Lamfers H-J, Meetsma A, Wiegiers G A and de Boer J L 1996 *J. Alloys Compounds* **241** 4418
- [5] van Landuyt J, Wiegiers G A and Amelinckx S 1978 *Phys. Status Solidi* **a 46** 479
- [6] Schwarz H G 1953 *Dissertation* Tübingen
- [7] van Bruggen C F, Haange R J, Wiegiers G A and de Boer D K G 1980 *Physica B* **99** 166
- [8] Tolsma P 1973 *Laboratory of Inorganic Chemistry, Internal Report, University of Groningen*  
Fang C M, Tolsma P R, van Bruggen C F, de Groot R A, Wiegiers G A and Haas C 1996 *J. Phys.: Condens. Matter* **8** 4381

- [9] Myron H W 1981 *Physica B* **105** 120
- [10] Yoshida Y and Motizuki K 1982 *J. Phys. Soc. Japan* **51** 2107
- [11] Zunger A and Freeman A J 1979 *Phys. Rev. B* **19** 6001
- [12] van Leuken H, Lodder A, Czyzyk M T, Springelkamp F and de Groot R A 1990 *Phys. Rev. B* **41** 5613
- [13] Hedin L and Lundqvist B I 1971 *J. Phys. C: Solid State Phys.* **4** 2064
- [14] Rigoult J, Guidi-Morosini C, Tomas A and Molinie P 1982 *Acta Crystallogr. B* **38** 1557
- [15] Anderson O K and Jepsen O 1984 *Phys. Rev. Lett.* **53** 2571
- [16] Riekel C 1976 *J. Solid State Chem.* **17** 389
- [17] Zunger A and Freeman A J 1978 *Phys. Rev. B* **17** 1839
- [18] Fang C M, de Groot R A and Haas C, to be published
- [19] Bongers P F, van Bruggen C F, Koopstra J, Omloo W P F A M, Wiegers G A and Jellinek F 1968 *J. Phys. Chem. Solids* **29** 977
- [20] van Laar B and Ijdo D J W 1971 *J. Solid State Chem.* **3** 590
- [21] van Laar B and Engelsman F M R 1971 *J. Solid State Chem.* **6** 384
- [22] Engelsman F M R, Wiegers G A, Jellinek F and van Laar B 1973 *J. Solid State Chem.* **6** 574
- [23] van Bruggen C F and Haas C 1976 *Solid State Commun.* **20** 251